Available online at www.sciencedirect.com
ScienceDirect
Applied Acoustics 68 (2007) 642–659
applied acoustics
www.elsevier.com/locate/apacoust

Optimal acoustic fields in compact thermoacoustic refrigerators

Gaelle Poignand [a], Bertrand Lihoreau [a], Pierrick Lotton [a,*], Etienne Gaviot [a], Michel Bruneau [a], Vitaly Gusev [b]

[a] *Laboratoire d'Acoustique de l'Université du Maine, UMR-CNRS 6613, Avenue O. Messiaen, 72085 Le Mans Cedex 09, France*
[b] *Laboratoire de Physique de l'Etat Condensé, UMR-CNRS 6687, Avenue O. Messiaen, 72085 Le Mans Cedex 09, France*

Received 5 September 2005; received in revised form 17 March 2006; accepted 20 March 2006
Available online 7 November 2006

Abstract

Thermoacoustic refrigerators have been developed during the last 15 years, employing quasi-standing resonant acoustic waves inside fluid-filled cavities to transfer heat along a stack region. Because higher efficiency can be reached when a significant travelling wave component exists in the resonator, specific resonant thermoacoustic devices have been designed allowing to adjust more or less the ratio of travelling and standing wave components. However, the acoustic pressure field and the particle velocity field do not appear to be the optimal ones, for the thermal quantities of interest. Thus, it is the aim of the paper to present a new kind of thermoacoustic standing wave-like device which allows to control easily and independently the pressure field and the particle velocity field, after investigating the optimal acoustic field, in the stack region, for the main parameters of interest, i.e. the temperature gradient, the thermoacoustic heat flow and the coefficient of performance.

Keywords: Thermoacoustics; Refrigerating systems; Miniaturisation

* Corresponding author. Tel.: +33 243 83 3270; fax: +33 243 83 3520.
E-mail address: pierrick.lotton@univ-lemans.fr (P. Lotton).

0003-682X/$ - see front matter © 2006 Elsevier Ltd. All rights reserved.
doi:10.1016/j.apacoust.2006.03.009

1. Introduction

Classical thermoacoustic refrigerators make generally use of quasi-standing acoustic waves to produce the work required to transfer heat from a cold heat exchanger to a hot one. Following Ceperley's ideas [1], travelling acoustic waves can also be used for thermoacoustic process [2]. Several works presented in the literature deal with the influence of standing wave ratio on this thermoacoustic process. Hofler [3] studied a standing wave thermoacoustic refrigerator and noted that higher efficiency can be reached when a significant travelling wave component is assumed. Raspet et al. [4] give the coefficient of performance of a thermoacoustic refrigerator as a function of the inverse of the standing wave ratio and confirm Hofler's conclusions. More recently, Petculescu and Wilen [5] designed a thermoacoustic device in which the ratio of travelling and standing waves components can be adjusted. All devices designed in the frame of these studies operate with a more or less controlled standing wave ratio in order to reach an optimum which is not clearly defined.

Therefore, the aim of this paper is twofold. Firstly, the optimal acoustic field in the stack region for thermoacoustic process in a standing wave-like refrigerator is investigated analytically, that is the optimal relationship between the acoustic pressure and the particle velocity is given, namely both their relative phase and their amplitude ratio. Secondly, a new kind of thermoacoustic device in which this optimal relationship between the acoustic pressure and the particle velocity can be obtained easily is described. Basic expressions of thermoacoustic quantities given in the literature are then rewritten in the first part of this paper (Section 2), emphasising separately the role played by the acoustic pressure p, the particle velocity u and their relative phase ϕ, and assuming that they are not linked anymore by standing wave conditions. Then, in a second part (Section 3), different optimal combinations of p, u and ϕ are found, respectively, for the main parameters of interest, i.e. the temperature gradient, the thermoacoustic heat flow and the coefficient of performance. The revisited description provides results showing that the characteristics of the optimal acoustic fields are not those of the usual half-wavelength resonator (Section 4). Nevertheless, for highest drive ratios, defined as the ratio of the acoustic pressure at the entrance of the resonator and the static pressure, standing wave refrigerators operate near the optimum in terms of particle velocity. However, some improvements can be achieved by tuning the relative phase between pressure and velocity to its optimum. The final part of this paper (Section 5) is devoted to the description of a non-half- (or quarter-) wavelength thermoacoustic device, designed in accordance with a recent patent requirements [6], in which the pressure field and the particle velocity field can be easily and independently controlled in order to create an optimal acoustic field and to monitor it during the process. Moreover, it must be emphasised that this new thermoacoustic refrigerator has the important advantage to be totally "compact", meaning that its dimensions are roughly those of the stack, heat exchangers and loudspeakers set very closed together. Finally, first experimental results are given which confirm that requirements that have to be taken into account in the design of thermoacoustic refrigerators can now be addressed, using theoretical results obtained in this work.

2. Expressions of thermoacoustic parameters as a function of the acoustic pressure, the particle velocity and their relative phase in the stack region

The literature abounds with many papers in which topics involving thermoacoustics processes are of principal focus (see Ref. [7] for example). But, to explain the general

subject matter of the paper, it is sufficient to review those which deal with the desired descriptors of the acoustic pressure and velocity fields of interest. Thermoacoustic process occurs inside a thermoacoustic core (a stack of plates or any equivalent porous material) when subjected to an acoustic wave. A schematic overall view of two plates of the stack considered in the following study is given in Fig. 1a and an expanded view is given in Fig. 1b. The thickness of each plate is denoted $2e_s$ and the thickness of each fluid layer $2y_0$. In a real thermoacoustic device, two heat exchangers are set at the ends of the stack. Acoustic plane waves produced in the stack region induce thermal interactions between gas and plates which lead to a hydrodynamical non-zero time-average heat transfer, denoted $\overline{Q}$, along the plates. This heat flow induces a temperature gradient, denoted $\partial_z T$, along the stack. The performance of the thermoacoustic process is given by the coefficient of performance (COP) defined as

$$\mathrm{COP} = \frac{\overline{Q}_\mathrm{c}}{\overline{W}}, \tag{1}$$

where $\overline{W}$ is the time-average acoustic power provided by the acoustic source and where $\overline{Q}_\mathrm{c}$ is the time-average heat flow extracted from the cold heat exchanger (one end of the stack), given by

$$\overline{Q}_\mathrm{c} = \overline{Q} - \overline{Q}_\mathrm{cond}, \tag{2}$$

$\overline{Q}_\mathrm{cond}$ being the heat flux due to axial heat conduction in the working fluid as well as in the stack plates.

Depending on the aimed application, one of these three quantities of interest (Q, $\partial_z T$ or COP) must be optimised. In the following, the analytical expressions of these thermoacoustic parameters are given as function of the acoustic pressure, the particle velocity and their relative phase considered as three independent variables, in order to determine the characteristics of the optimal acoustic field for a given application.

The z-component $u_z(x, y)$ of the particle velocity between two plates of the stack (Fig. 1), function of the acoustic pressure gradient, is given by [7]

$$u_z(y,z) = \frac{\mathrm{i}}{\rho_0 \omega}\left(1 + \frac{e_s}{y_0}\right)\frac{\partial p(z)}{\partial z}\left(1 - \frac{\cosh[(1+\mathrm{i})y/\delta_v]}{\cosh[(1+\mathrm{i})y_0/\delta_v]}\right), \tag{3}$$

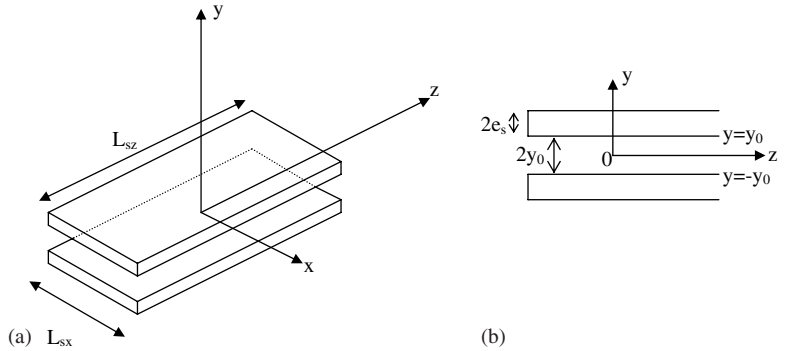

Fig. 1. Schematic view of two plates of the stack: (a) overall view; (b) expended view.

where ω is the angular frequency, ρ_0 is the mean density of the fluid and where $\delta_v = \sqrt{\frac{2\mu}{\rho_0\omega}}$ is the viscous penetration depth, μ being the shear viscosity coefficient.

Expression (3) is written here

$$u_z(y,z) = \frac{u}{(1-f_v)}\left(1 - \frac{\cosh[(1+\mathrm{i})y/\delta_v]}{\cosh[(1+\mathrm{i})y_0/\delta_v]}\right), \tag{4}$$

where

$$f_v = \frac{\tanh[(1+\mathrm{i})y_0/\delta_v]}{(1+\mathrm{i})y_0/\delta_v} \tag{5}$$

is a function which takes into account the effect of the viscosity on the particle velocity, and where

$$u = \frac{1}{y_0}\int_0^{y_0} u_z(y,z)\,\mathrm{d}z = (1-f_v)\left(1+\frac{e_s}{y_0}\right)\frac{\mathrm{i}}{\rho_0\omega}\frac{\partial p(z)}{\partial z}, \tag{6}$$

is the mean velocity across the thickness of the fluid layer between the plates.

In order to introduce the relative phase ϕ between the particle velocity and the acoustic pressure,

$$\phi = \phi_u - \phi_p, \tag{7}$$

the mean particle velocity is written

$$u = |u|\,\mathrm{e}^{\mathrm{i}\phi}, \tag{8}$$

and p is considered as positive real function.

On the other hand, the oscillating temperature $\tau(y,z)$ between two plates of the stack is written [7]

$$\begin{aligned}\tau(y,z) = {} & \frac{T_0\alpha}{\rho_0 C_p}p\left(1 - \frac{\cosh[(1+\mathrm{i})y/\delta_h]}{\cosh[(1+\mathrm{i})y_0/\delta_h]}\right) + \mathrm{i}\frac{u}{(1-f_v)\omega} \\ & \times \frac{\partial T_0}{\partial z}\left(1 - \frac{\sigma\cosh[(1+\mathrm{i})y/\delta_v]}{(\sigma-1)\cosh[(1+\mathrm{i})y_0/\delta_v]} + \frac{\cosh[(1+\mathrm{i})y/\delta_h]}{(\sigma-1)\cosh[(1+\mathrm{i})y_0/\delta_h]}\right),\end{aligned} \tag{9}$$

where T_0 is the mean temperature, C_p its constant-pressure heat capacity per unit mass, α its thermal expansion coefficient, σ the Prandtl number and where $\delta_h = \sqrt{\frac{2K}{\rho_0 C_p \omega}}$ is the thermal penetration depth, K being the diffusive thermal conductivity of the fluid.

2.1. Thermoacoustic heat flux

When assuming the classical hypotheses used in linear thermoacoustic theory (quasi-plane wave approximation, short stack approximation, working gas assumed to be an ideal gas, no temperature dependance of the thermo-physical properties of the fluid and the plates, large heat capacity per unit area of the plates, mean temperature in the fluid equal to the mean temperature of the plates and independent of the y-coordinate normal to the plate), the time-average thermoacoustic heat flux per unit area $\bar{q}$ along the z-axis is written as [7]

$$\bar{q} = \frac{1}{2}\rho_0 C_p \Re(\tau u_z^*) - \frac{1}{2}T_O\alpha\Re(pu_z^*), \tag{10}$$

$\Re(\,)$ standing for the real part and $*$ denoting the complex conjugate. In the basic thermoacoustic theory, the second term of the right hand side of Eq. (10) vanishes because p and u_z are out of phase in time (pure standing wave). This hypothesis is no longer assumed in this paper.

Combining Eq. (10) and the expressions (4) and (9) for the z-component of the particle velocity and the oscillating temperature, respectively, the total time-average heat flux $\overline{Q}$ in the z-direction, given by

$$\overline{Q} = 2\int_0^{L_{sx}}\int_0^{y_0} \bar{q}\,\mathrm{d}x\,\mathrm{d}y, \tag{11}$$

can be written

$$\overline{Q} = \frac{L_{sx}y_0T_0\alpha}{(1+\sigma)}\Re\left[pu^*\frac{f_v^*-f_h}{(1-f_v^*)}\right] + \frac{L_{sx}y_0}{(1-\sigma^2)}\frac{C_p\rho_0}{\omega}|u|^2\Im\left[\frac{f_h+\sigma f_v^*}{(1-f_v^*)(1-f_v)}\right]\frac{\partial T_0}{\partial z} \tag{12}$$

where $\Im(\,)$ stands for the imaginary part, L_{sx} is the width of a plate in the x-direction, and

$$f_h = \frac{\tanh[(1+\mathrm{i})y_0/\delta_h]}{(1+\mathrm{i})y_0/\delta_h} \tag{13}$$

is a function which takes into account the effects of thermal conduction.

Assuming the so-called boundary layer approximation, that is $y_0 \geqslant 2\delta_{h,v}$ (approximation easily assumed for standing wave-like thermoacoustic devices), then $\tanh[(1+i)y_0/\delta_{h,v}] \approx 1$ [7] and the relationship (12) becomes

$$\overline{Q} = \frac{\delta_h L_{sx}}{2\left(1-\frac{\delta_v}{y_0}+\frac{\delta_v^2}{2y_0^2}\right)}\left\{\frac{T_0\alpha}{(1+\sigma)}\Re\left(pu^*\left[\left(-1+\sqrt{\sigma}-\frac{\delta_v}{y_0}\sqrt{\sigma}\right)\right.\right.\right.$$
$$\left.\left.\left.+\mathrm{i}\left(1+\sqrt{\sigma}-\frac{\delta_v}{y_0}\right)\right]\right) - \frac{(1-\sigma\sqrt{\sigma})}{(1-\sigma^2)}\frac{C_p\rho_0}{\omega}|u|^2\frac{\partial T_0}{\partial z}\right\}. \tag{14}$$

Then, using Eqs. (7) and (8) the total heat flux is given by

$$\overline{Q} = \frac{\delta_h L_{sx}}{2\left(1-\frac{\delta_v}{y_0}+\frac{\delta_v^2}{2y_0^2}\right)}\left\{\frac{T_0\alpha p|u|}{(1+\sigma)}\left[\left(-1+\sqrt{\sigma}-\frac{\delta_v}{y_0}\sqrt{\sigma}\right)\cos\phi\right.\right.$$
$$\left.\left.+\left(1+\sqrt{\sigma}-\frac{\delta_v}{y_0}\right)\sin\phi\right] - \frac{(1-\sigma\sqrt{\sigma})}{(1-\sigma^2)}\frac{C_p\rho_0}{\omega}|u|^2\frac{\partial T_0}{\partial z}\right\}. \tag{15}$$

In this relationship, which is equivalent to Eq. (12) in Ref. [8], the hydrodynamical heat flux is expressed as a sum of two terms, respectively, proportional to $p|u|$ and $|u|^2$. The first term gives the heat flow in absence of a longitudinal temperature gradient, and the second one, which accounts for the so-called "acoustically induced thermal conductivity" effect [9], represents a heat flow which propagates in the opposite direction of the preceding one and then which diminishes the efficiency of the thermoacoustic process.

2.2. Temperature gradient

An estimation of the upper limit of the temperature gradient $\partial_z T$ which can be ideally reached in steady-state regime is obtained when assuming that no heat exchangers are set at the end of the stack of plates. So, the heat flow $\overline{Q}_c$ extracted from the cold heat exchanger vanishes and then, neglecting any heat losses in the system, the thermoacoustically induced

heat flux $\overline{Q}$ in the gas is entirely balanced by the conductive heat flux in the opposite direction $\overline{Q}_{\text{cond}}$ (due to the diffusive conduction through the plates and through the gas) given by [10]

$$\overline{Q}_{\text{cond}} = -2L_{sx}(Ky_0 + K_s e_s)\frac{\partial T_0}{\partial z}, \tag{16}$$

K_s being the diffusive thermal conductivity of the plates. Thus, assuming classical hypotheses listed in the previous section and boundary layer approximation, the relationship (2) leads to the following expression for the temperature gradient [10]:

$$\frac{\partial T_0}{\partial z} = \frac{\dfrac{\delta_h T_0 \alpha}{4(1+\sigma)\left(1-\frac{\delta_v}{y_0}+\frac{\delta_v^2}{2y_0^2}\right)}\Re\left(pu^*\left[\left(-1+\sqrt{\sigma}-\dfrac{\delta_v}{y_0}\sqrt{\sigma}\right)+\mathrm{i}\left(1+\sqrt{\sigma}-\dfrac{\delta_v}{y_0}\right)\right]\right)}{(Ky_0+K_s e_s)+\frac{\delta_h}{4}\dfrac{1-\sigma\sqrt{\sigma}}{(1-\sigma^2)\left(1-\frac{\delta_v}{y_0}+\frac{\delta_v^2}{2y_0^2}\right)}\dfrac{C_p\rho_0}{\omega}|u|^2}. \tag{17}$$

Using expression (8) for the mean particle velocity, Eq. (17) becomes

$$\frac{\partial T_0}{\partial z} = \frac{\delta_h T_0 \alpha p|u|}{4(1+\sigma)\left(1-\frac{\delta_v}{y_0}+\frac{\delta_v^2}{2y_0^2}\right)}\frac{\left(-1+\sqrt{\sigma}-\frac{\delta_v}{y_0}\sqrt{\sigma}\right)\cos\phi+\left(1+\sqrt{\sigma}-\frac{\delta_v}{y_0}\right)\sin\phi}{(Ky_0+K_s e_s)+\frac{\delta_h}{4}\dfrac{1-\sigma\sqrt{\sigma}}{(1-\sigma^2)\left(1-\frac{\delta_v}{y_0}+\frac{\delta_v^2}{2y_0^2}\right)}\dfrac{C_p\rho_0}{\omega}|u|^2}. \tag{18}$$

2.3. Coefficient of performance

The expression of time-average acoustic work $\overline{W}$ which appears in the expression COP of the coefficient of performance is written here as [7]

$$\overline{W} = \frac{L_{sx}L_{sz}\delta_h}{2}\left\{-\frac{\omega(\gamma-1)}{\rho_0 c_0^2}|p|^2+\alpha p|u|\frac{\partial T_0}{\partial z}\left[\frac{\left(1-\sqrt{\sigma}-\frac{\delta_v}{y_0}+\sqrt{\sigma}\frac{\delta_v}{y_0}\right)\cos\phi+(1-\sqrt{\sigma})\sin\phi}{(1-\sigma)\left(1-\frac{\delta_v}{y_0}+\frac{\delta_v^2}{2y_0^2}\right)}\right]\right.$$
$$\left.-\frac{\sqrt{\sigma}\omega\rho_0|u|^2}{1-\frac{\delta_v}{y_0}+\frac{\delta_v^2}{2y_0^2}}\right\}. \tag{19}$$

An estimation of the upper limit of the heat flow $\overline{Q}_c$ which can be ideally extracted from the cold heat exchanger is obtained when assuming that the conductive heat flow along the stack of plates is negligible, that is when assuming that $\overline{Q}_{\text{cond}}$ vanishes in Eq. (2). So, the heat flow $\overline{Q}_c$ extracted from the cold heat exchanger is equal to the thermoacoustic heat flux $\overline{Q}$, and the upper limit of the coefficient of performance (COP) is then the ratio of the expressions (15) and (19) of the thermoacoustic heat flux and the acoustic work, respectively, namely

$$\text{COP} = \frac{\left\{\frac{T_0\alpha p|u|}{(1+\sigma)}\left[\left(-1+\sqrt{\sigma}-\frac{\delta_v}{y_0}\sqrt{\sigma}\right)\cos\phi+\left(1+\sqrt{\sigma}-\frac{\delta_v}{y_0}\right)\sin\phi\right]-\frac{(1-\sigma\sqrt{\sigma})}{(1-\sigma^2)}\frac{C_p\rho_0}{\omega}|u|^2\frac{\partial T_0}{\partial z}\right\}}{L_{sz}\left\{-\frac{\omega(\gamma-1)}{\rho_0 c_0^2}\left(1-\frac{\delta_v}{y_0}+\frac{\delta_v^2}{2y_0^2}\right)|p|^2+\frac{\partial T_0}{\partial z}\frac{\left(1-\frac{\delta_v}{y_0}\right)\cos\phi+\sin\phi}{(1+\sqrt{\sigma})}\alpha p|u|-\sqrt{\sigma}\omega\rho_0|u|^2\right\}}. \tag{20}$$

3. Optimal acoustic fields for thermoacoustic quantities of interest

Optimal relationships between p, $|u|$ and ϕ which provide the maximal value of each quantity of interest can easily be derived from relations (15), (18) and (20). They are given in the following, respectively, for the temperature gradient $\partial_z T$, the heat flux $\overline{Q}$ and the coefficient of performance (COP)

According to linear theory, an acoustic pressure level as high as possible is obviously required to maximise the temperature gradient, because this gradient is proportional to the amplitude of the acoustic pressure (Eq. (18)). Therefore, optimal value for the amplitude of the particle velocity (which is different to its maximal value) and optimal value of the relative phase can be found to maximise the temperature gradient. The temperature gradient $\partial_z T$ (Eq. (18)) is expressed as a product of two functions, one depending only on the variable $|u|$ and one depending only on the variable ϕ. Thus, after deriving independently with respect to variables $|u|$ and ϕ, the maximum value of the temperature gradient is obtained when these variables are given separately by

$$|u|_{\text{opt}} = \sqrt{\frac{4\omega(Ky_0 + K_s e_s)(1-\sigma^2)\left(1 - \frac{\delta_v}{y_0} + \frac{\delta_v^2}{2y_0^2}\right)}{\delta_h \rho_0 C_p (1 - \sigma\sqrt{\sigma})}}, \tag{21}$$

and

$$\phi_{\text{opt}} = \arctan\left(-\frac{1 + \sqrt{\sigma} - \frac{\delta_v}{y_0}}{1 - \sqrt{\sigma} + \frac{\delta_v}{y_0}\sqrt{\sigma}}\right) + n\pi. \tag{22}$$

These optimal values depend on the frequency, on the shape and the dimensions of the stack, and on the thermo-physical properties of the fluid and the plates. For an inviscid fluid ($\sigma = 0$, $\delta_v = 0$), the optimal relative phase is $\phi_{\text{opt}} = -\frac{\pi}{4}$ or $\phi_{\text{opt}} = \frac{3\pi}{4}$. For a viscous fluid, the optimal phase is close, but different, to the phase ϕ_r of a pure standing wave ($\phi_r \approx \pm\frac{\pi}{2}$).

As an example, Fig. 2 shows the theoretical temperature gradient, normalised by its maximum value, as function of the amplitude and the relative phase of the particle velocity in the stack region, normalised by their optimal values, for a given set of thermo-physical and geometrical parameters of the stack (Table 1). As expected, maximal value of temperature gradient is obtained when the amplitude and the phase of the particle velocity reach their optimal values simultaneously.

Substituting the expression (18) of the temperature gradient $\partial_z T$ in the expression (15) of the heat flow $\overline{Q}$ leads to

$$\begin{aligned}\overline{Q} = {} & \frac{\delta_h L_{sx} T_0 \alpha p |u|}{2(1+\sigma)\left(1 - \frac{\delta_v}{y_0} + \frac{\delta_v^2}{2y_0^2}\right)} \\ & \times \frac{(Ky_0 + K_s e_s)\left[\left(-1 + \sqrt{\sigma} - \frac{\delta_v}{y_0}\sqrt{\sigma}\right)\cos\phi + \left(1 + \sqrt{\sigma} - \frac{\delta_v}{y_0}\right)\sin\phi\right]}{(Ky_0 + K_s e_s) + \frac{\delta_h}{4}\frac{1-\sigma\sqrt{\sigma}}{(1-\sigma^2)\left(1 - \frac{\delta_v}{y_0} + \frac{\delta_v^2}{2y_0^2}\right)}\frac{C_p \rho_0}{\omega}|u|^2}.\end{aligned} \tag{23}$$

Then, after deriving the expression (23) independently with respect to variables $|u|$ and ϕ, it follows that the optimal value $|u|_{\text{opt}}$ of the amplitude of the particle velocity and the opti-

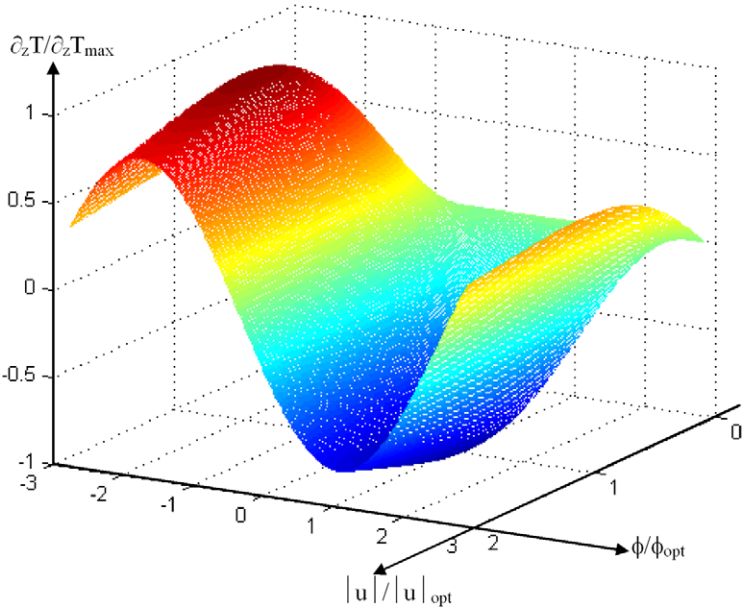

Fig. 2. Normalised temperature gradient as a function of normalised amplitude of particle velocity and normalised phase between particle velocity and acoustic pressure. Geometrical and thermo-physical parameters are given in Table 1.

Table 1
Geometrical and physico-thermal parameters of the thermoacoustic device

Working fluid	Air
Working frequency (Hz)	$f = 160$
Static pressure level (Pa)	$P_0 = 1.013 \times 10^5$
Mean operating temperature (K)	$T_0 = 295$
Stack material	
Stack length (m)	$L_{sz} = 19 \times 10^{-2}$
Stack width (m)	$L_{sx} = 19 \times 10^{-2}$
Plate thickness (m)	$2e_s = 2 \times 10^{-3}$
Plate spacing (m)	$2y_0 = 610 \times 10^{-6}$
Mean density (kg m^{-3})	$\rho_s = 1400$
Specific heat (J kg^{-1} K^{-1})	$C_s = 2300$
Thermal conductivity (W m^{-1} K^{-1})	$K_s = 0.19$

mal value ϕ_{opt} of the phase ϕ is given here by the same relationships as the ones obtained above (Eqs. (21) and (22)). The same results as those shown in Fig. 2 are obtained when representing the theoretical thermoacoustic heat flux, normalised by its maximum value, as function of the amplitude and the relative phase of the particle velocity in the stack region, normalised by their optimal values.

The optimal field for the coefficient of performance cannot be obtained as simply as the preceding ones. Then, results are given by way of an example rather than attempt a general treatment of the optimisation of the COP. This example is given in Fig. 3 which shows the theoretical coefficient of performance as a function of the amplitude (normalised by the

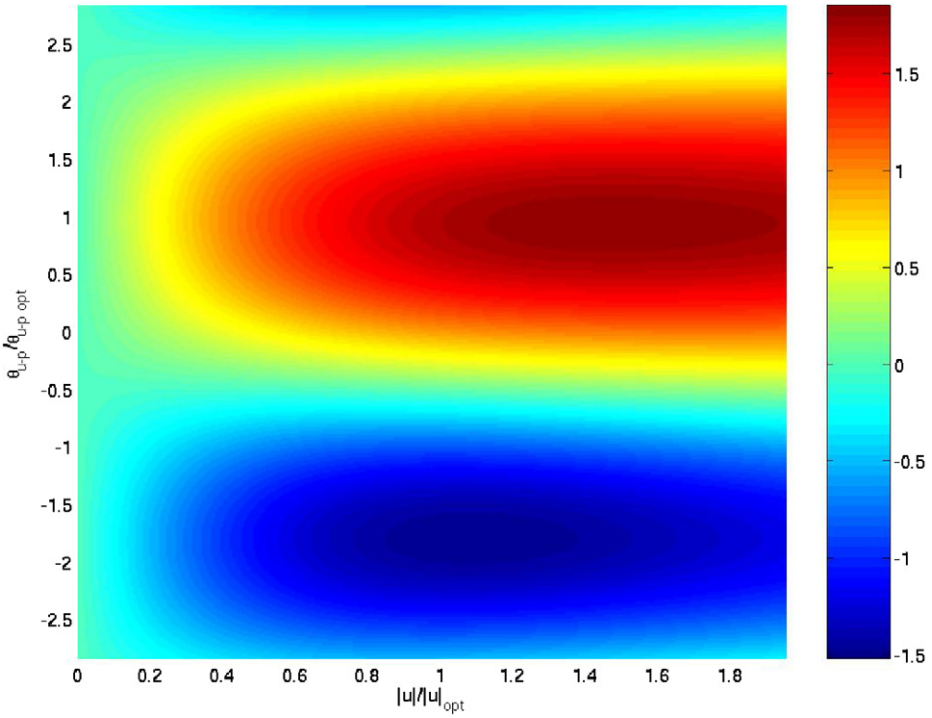

Fig. 3. Coefficient of performance as a function of amplitude of particle velocity (normalised by the optimal value given by Eq. (21)) and phase between particle velocity and acoustic pressure (normalised by the optimal value given by Eq. (22)), for a given drive ratio (1.5%), and for a given temperature gradient along the stack ($\partial_z T = 100\ \mathrm{K\ m^{-1}}$). Geometrical and thermo-physical parameters are given in Table 1.

optimal value defined by Eq. (21)) and the relative phase (normalised by the optimal value defined by Eq. (22)) of the particle velocity in the stack region, considering the set of parameters of Table 1. In this example, the drive ratio is set at 1.5% and the temperature gradient is set in such a way that it leads to a temperature difference of 20 K between the ends of the stack ($\partial_z T = 100\ \mathrm{K\ m^{-1}}$), which corresponds to the operating temperature range of a typical household refrigerator. Maximal value of COP is obtained for values of the amplitude and the phase of the particle velocity slightly different than optimal values given in Eqs. (21) and (22).

4. Comparison between standing wave and optimal acoustic field refrigerators

As mentioned above, the so-called optimal fields may be advantageous in the optimisation of the characteristics of the thermoacoustic quantities of interest. In order to characterise this optimisation, a theoretical comparison with the performances which rely on usual half-wavelength thermoacoustic resonators is presented in this section.

The operation of classical thermoacoustic refrigerators employs acoustic fields inside fluid-filled half-wavelength resonant closed tubes (Fig. 4) to create a heat flux along a short stack or an equivalent porous materials (short meaning that the length of the stack is much smaller than the acoustic wavelength). Assuming that the stack does not perturb the standing wave appreciably, the acoustic pressure can be written

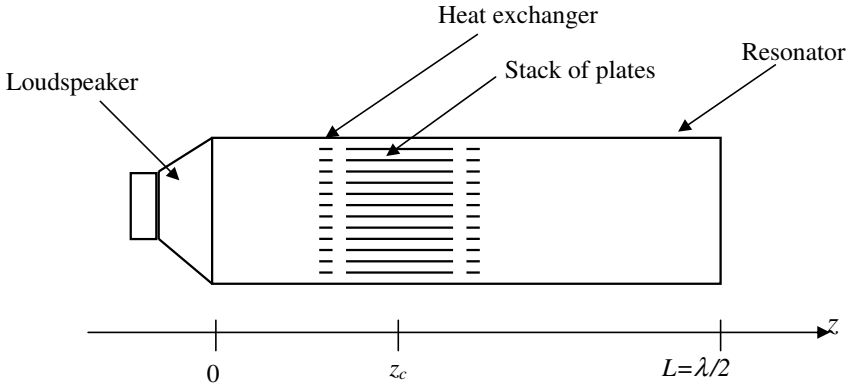

Fig. 4. Schematic view of a classical standing wave thermoacoustic refrigerator.

$$p = P_A \cos(k_0 z), \tag{24}$$

with $k_0 = \frac{\omega}{c_0}$. Given the specificity of the aim of the paper, the correction of the length of the resonator due to coupling with the acoustic source [11] is neglected below. Combining this expression of the acoustic pressure field and Eq. (7) leads to the mean particle velocity u_r across the fluid layer between two adjacent plates in a standing wave resonator

$$u_r = -\mathrm{i}(1 - f_v)\left(1 + \frac{e_s}{y_0}\right)\frac{P_A}{\rho_0 c_0}\sin(k_0 z_c), \tag{25}$$

where z_c is the co-ordinate of the centre of the stack in the resonator. In the frame of the boundary layer approximation, this expression becomes

$$u_r = \left[\frac{\delta_v}{2y_0} + \mathrm{i}\left(\frac{\delta_v}{2y_0} - 1\right)\right]\left(1 + \frac{e_s}{y_0}\right)\frac{P_A}{\rho_0 c_0}\sin(k_0 z_c). \tag{26}$$

The relative phase ϕ_r between the mean particle velocity and the acoustic pressure is close (but not equal) to $-\frac{\pi}{2}$ for $0 \leqslant z_c \leqslant \frac{\lambda}{4}$ $\left(\phi_r = \mathrm{arctg}\left(1 - \frac{2y_0}{\delta_v}\right)\right)$ and close (but not equal) to $\frac{\pi}{2}$ for $\frac{\lambda}{4} \leqslant z_c \leqslant \frac{\lambda}{2}$ $\left(\phi_r = \mathrm{arctg}\left(1 - \frac{2y_0}{\delta_v}\right) - \pi\right)$. Then Eqs. (15), (18) and (20) lead, respectively, to

$$\begin{aligned}\overline{Q}^{\mathrm{s}}(z_c) = {} & \frac{\delta_h L_{sx}}{4\rho_0 c_0} P_A^2 \left(1 + \frac{e_S}{y_0}\right)\left\{-\frac{1 - \sigma\sqrt{\sigma}}{1 - \sigma^2}\frac{C_p}{\omega c_0}\left(1 + \frac{e_S}{y_0}\right)\partial_z T_0 (1 - \cos(2k_0 z_c))\right. \\ & + \frac{\alpha T_0}{(1+\sigma)\sqrt{1 - \frac{\delta_v}{y_0} + \frac{\delta_v^2}{2y_0^2}}}\sin(2k_0 z_c)\left[\left(-1 + \sqrt{\sigma} - \frac{\delta_v}{y_0}\sqrt{\sigma}\right)\cos\phi_r\right. \\ & \left.\left. + \left(1 + \sqrt{\sigma} - \frac{\delta_v}{y_0}\right)\sin\phi_r\right]\right\},\end{aligned} \tag{27}$$

$$\begin{aligned}\frac{\partial T_0^{\mathrm{s}}}{\partial z}(z_c) = {} & \frac{\delta_h T_0 \alpha P_A^2 \left(1 + \frac{e_s}{y_0}\right)\sin(2k_0 z_c)}{8(1+\sigma)\rho_0 c_0 \sqrt{1 - \frac{\delta_v}{y_0} + \frac{\delta_v^2}{2y_0^2}}} \\ & \times \frac{\left(-1 + \sqrt{\sigma} - \frac{\delta_v}{y_0}\sqrt{\sigma}\right)\cos\phi_r + \left(1 + \sqrt{\sigma} - \frac{\delta_v}{y_0}\right)\sin\phi_r}{(Ky_0 + K_s e_s) + \frac{\delta_h}{8}\frac{1 - \sigma\sqrt{\sigma}}{(1-\sigma^2)}\frac{C_p P_A^2}{\omega\rho_0 c_0^2}\left(1 + \frac{e_s}{y_0}\right)^2 [1 - \cos(2k_0 z_c)]},\end{aligned} \tag{28}$$

and

$$\mathrm{COP}^{\mathrm{s}} = \frac{\left(1+\frac{e_s}{y_0}\right)}{L_{sy}}\left\{\frac{T_0\alpha}{1+\sigma}\sin(2k_0z_c)\left[\left(-1+\sqrt{\sigma}-\frac{\delta_v}{y_0}\sqrt{\sigma}\right)\cos\phi_r+\left(1+\sqrt{\sigma}-\frac{\delta_v}{y_0}\right)\sin\phi_r\right]\right.$$
$$\left.-\frac{C_p}{\omega c_0}\left(1+\frac{e_s}{y_0}\right)\frac{1-\sigma\sqrt{\sigma}}{1-\sigma^2}\sqrt{1-\frac{\delta_v}{y_0}+\frac{\delta_v^2}{2y_0^2}}\partial_z T_0(1-\cos(2k_0z_c))\right\}$$
$$\times\left\{-\frac{\omega}{c_0}\sqrt{1-\frac{\delta_v}{y_0}+\frac{\delta_v^2}{2y_0^2}}\left[\cos(2k_0z_c)\left(\gamma-1-\left(1+\frac{e_s}{y_0}\right)^2\sqrt{\sigma}\right)\right.\right.$$
$$\left.\left.+\left(\gamma-1+\left(1+\frac{e_s}{y_0}\right)^2\sqrt{\sigma}\right)\right]+\left(1+\frac{e_s}{y_0}\right)\frac{\alpha}{1+\sqrt{\sigma}}\left[\left(1-\frac{\delta_v}{y_0}\right)\cos\phi_r+\sin\phi_r\right]\partial_z T_0\sin(2k_0z_c)\right\}^{-1}. \tag{29}$$

where the superscript s refers to standing waves.

The comparison between the behaviour of a usual half-wavelength thermoacoustic refrigerator and the behaviour of a thermoacoustic refrigerator in which pressure and velocity can be independently controlled is limited below to the behaviour of the temperature gradient (thereby, supporting the method which can easily be extrapolated to the other quantities of interest).

Being concerned first by the evolution of the temperature gradient as function of the acoustic pressure level, and then involving Eq. (18), along with Eqs. (21) and (22), and Eq. (28), we consider here the two following situations:

(i) first, the stack is set in an acoustical field tuned in such a way that the amplitude of the particle velocity is the theoretical optimal one ($|u| = |u|_{\mathrm{opt}}$) and that the relative phase corresponds to the resonance of a standing wave ($\phi = \phi_r = \mathrm{arctg}\left(1-\frac{2y_0}{\delta_v}\right)$), the amplitude of the particle velocity and the phase of the particle velocity being not dependant on the acoustic pressure p,
(ii) second, the stack is located at a fixed position $z_c = \lambda/8$ in a standing wave resonator, the amplitude and the phase of the particle velocity being then set to $|u| = |u_r|$ and $\phi = \phi_r$, respectively.

The theoretical results for the temperature gradient as function of the pressure level in the stack are shown in Fig. 5. For a given acoustic pressure level, the values of the temperature gradient when $|u| = |u|_{\mathrm{opt}}$ are always greater than its values when $|u| = |u_r|$ (half-wavelength resonator), except when $|u_r| = |u|_{\mathrm{opt}}$ (they are equal).

Nevertheless, as mentioned in the previous section, the highest acoustic pressure level is required to maximise the temperature gradient. In this situation, the amplitude of the particle velocity $|u_r|$ inside a stack located at a position $z_c = \lambda/8$ in a standing wave resonator is greater than the optimal amplitude of the particle velocity $|u_{\mathrm{opt}}|$. Therefore, setting the stack centre closer to the acoustic source ($z_c < \frac{\lambda}{8}$, see Fig. 4) in the half-wavelength resonator, the acoustic pressure increases and the particle velocity $|u_r|$ decreases towards the optimal value $|u|_{\mathrm{opt}}$. The normalised co-ordinate $\eta_u = \frac{z_u}{\lambda}$ corresponding to the position in the resonator for which the velocity $|u_r| = |u|_{\mathrm{opt}}$ is shown in Fig. 6 as function of the drive ratio (DR). For the lowest values of the acoustic pressure, this co-ordinate η_u does not exist because the value of $|u_r|$ cannot reach the value of $|u|_{\mathrm{opt}}$. Such a discussion has a marked

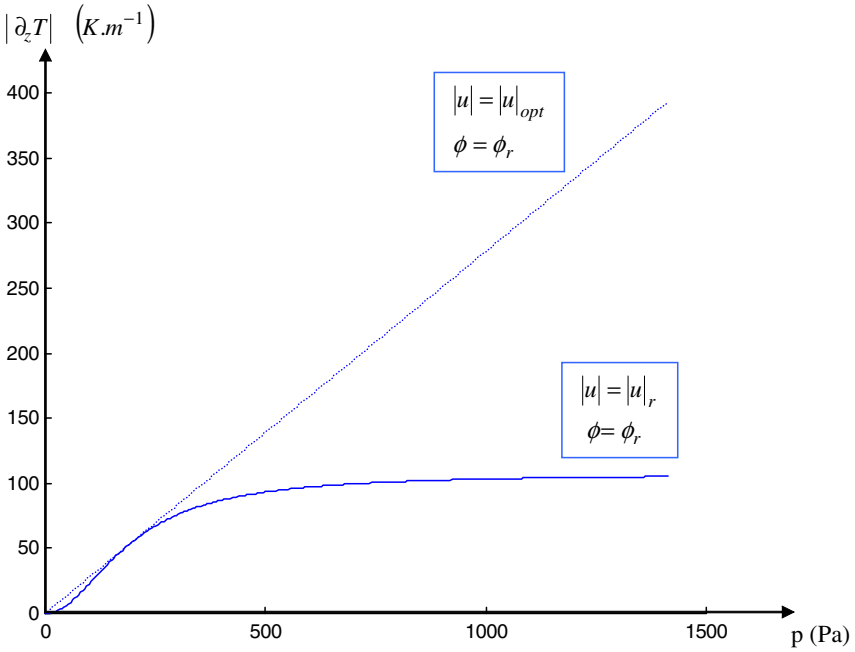

Fig. 5. Temperature gradient along the stack as a function of acoustic pressure level, for geometrical and thermophysical parameters given in Table 1. (Straight line) The stack is located at the quarter of the length of the resonator; the amplitude of the particle velocity (which depends on the acoustic pressure level) and its phase are the ones existing in a standing wave resonator ($|u| = |u|_r$ and $\phi = \phi_r$). (Dotted line) the stack is set in an acoustic field tuned in such a way that the amplitude of the particle velocity is fixed at its optimal value (and then does not depend on the acoustic pressure level) and that its phase is the one existing in a standing wave resonator ($|u| = |u|_{\text{opt}}$ and $\phi = \phi_r$).

shortcoming, however, since the maximum temperature gradient which can be reached in a half-wavelength resonator involves the complex expression (28). Thus, by setting the derivative of the expression (28) with respect to the co-ordinate z_c equal to zero, there follows an optimal stack centre position function $(z_c)_{\text{opt}}$ in the half-wavelength resonator:

$$(z_c)_{\text{opt}} = \frac{1}{2k_0} \arccos \left\{ \frac{\frac{\delta_h}{8} \frac{1-\sigma\sqrt{\sigma}}{(1-\sigma^2)} \frac{C_p P_a^2}{\omega \rho_0 c_0^2} \left(1 + \frac{e_s}{y_0}\right)^2}{[K y_0 + K_s e_s] + \frac{\delta_h}{8} \frac{1-\sigma\sqrt{\sigma}}{(1-\sigma^2)} \frac{C_p P_a^2}{\omega \rho_0 c_0^2} \left(1 + \frac{e_s}{y_0}\right)^2} \right\}. \tag{30}$$

For a standing wave refrigerator the parameters of which are given in Table 1, the optimal normalised co-ordinate of the centre of the stack $(z_c)_{\text{opt}}/\lambda$ is shown in Fig. 6, as function of the drive ratio. It is noteworthy that $(z_c)_{\text{opt}} \to 0$ when the acoustic level increases (i.e. the stack is very close to the acoustic source, near the maximum value of the acoustic pressure in the standing wave). This property was previously mentioned, both from experiments [8] and from analytical model [10]. For the highest acoustic levels, that is for drive ratios greater than 1%, the value of the modulus of the particle velocity $|u_r|$ can be equal to the optimal value $|u|_{\text{opt}}$ when the stack centre is set at its optimal value $(z_c)_{\text{opt}}$. This result means that a usual half-wavelength standing wave refrigerator operates near the optimum in terms of the modulus of the particle velocity when a high drive ratio is reached. But, as

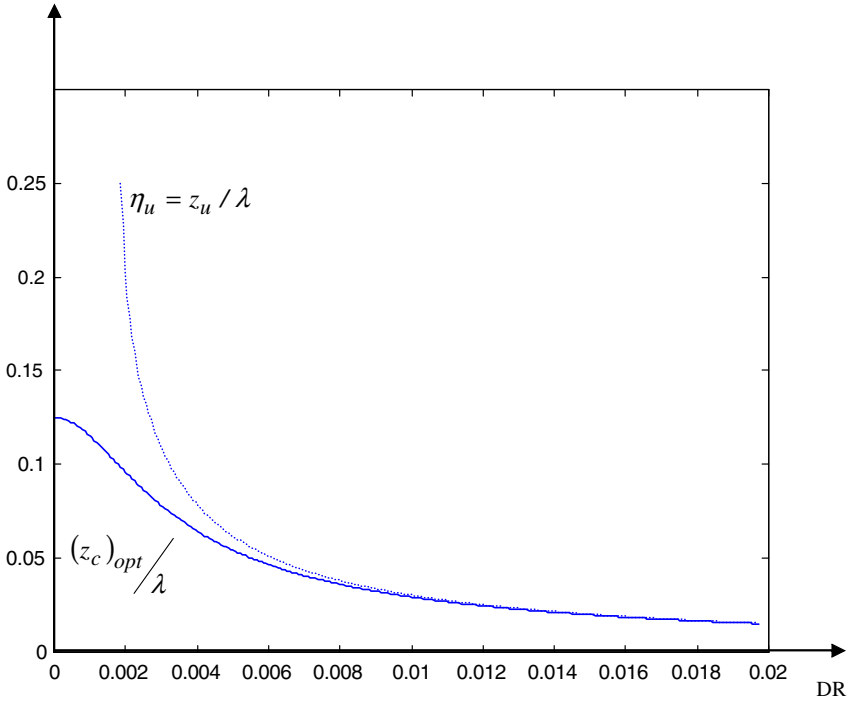

Fig. 6. (Dotted line) Normalised co-ordinate $\eta_u = \frac{z_u}{\lambda}$, corresponding to the position in the standing wave resonator (Table 1) for which the velocity $|u_r| = |u|_{\text{opt}}$, as function of the drive ratio (DR). (Straight line) Optimal normalised co-ordinate of the centre of the stack $(z_c)_{\text{opt}}/\lambda$, corresponding to the position in the standing wave resonator (Table 1) for which the temperature gradient is maximum, as a function of the drive ratio.

regards to lower drive ratios which can occurs for example when trying to miniaturise thermoacoustic half-wavelength resonators, Fig. 6 readily shows that the value of $|u|_r$ cannot reach the optimal value $|u|_{\text{opt}}$. This result should be of interest when designing such thermoacoustic refrigerators. Moreover, for any value of the acoustic pressure level in half-wavelength resonators, some improvements would be achieved by tuning the relative phase between acoustic pressure and particle velocity to its optimum.

The complete determination of the optimal acoustic field implies that the values of both $|u|_{\text{opt}}$ and ϕ_{opt} are given independently by Eqs. (24) and (25), involving an acoustic field different from a pure half-wavelength resonant field (in particular, $\phi_{\text{opt}} \neq \frac{\pi}{2}$). This would be achieved using other kinds of resonators than cylindrical waveguides. The thermoacoustic device presented in the next section permits creation of the acoustic field expected here.

5. Experimental results

A new kind of thermoacoustic device has been designed in accordance with recent patent requirements [6]. A schematic view of this device is given in Fig. 7. It is a non-resonant thermoacoustic device in which the resonator is replaced by a cavity fitting the dimensions of the stack. The acoustic pressure and the particle velocity are generated in the stack by a set of loudspeakers: one loudspeaker or a couple of face-to-face loudspeakers (supplied

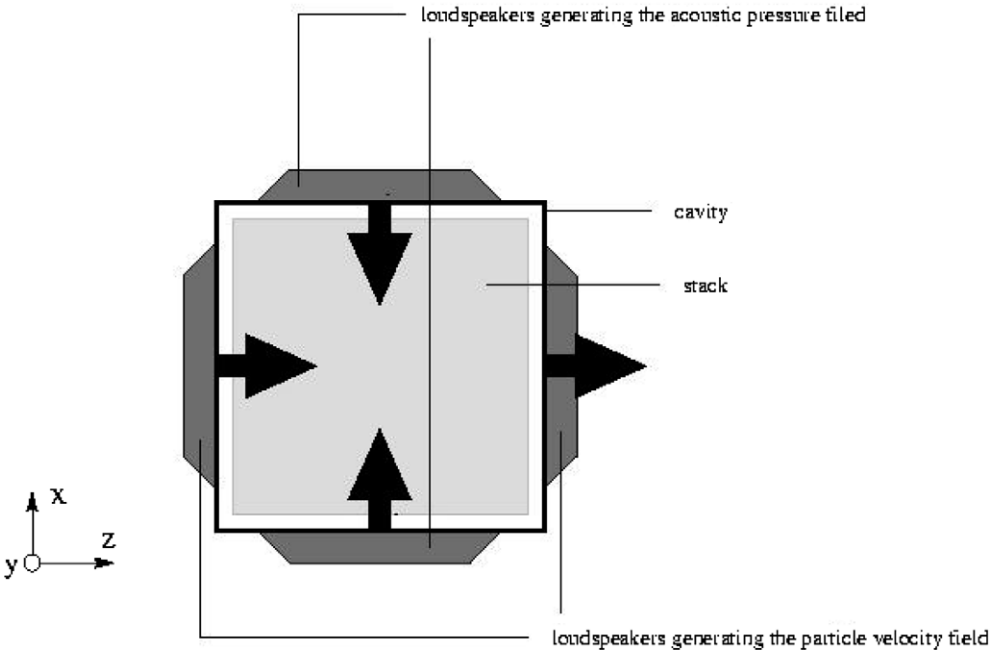

Fig. 7. Schematic view of the "compact" device. The arrows represent the relative displacements of two face to face acoustic sources during a half-sine.

with electrical voltages in phase) generates the pressure field in the cavity, while another couple (supplied with electrical voltages $\pi/2$ out of phase) generates the particle velocity field along the z-axis. The acoustic pressure and the particle velocity are not linked anymore by standing wave or travelling wave conditions, and can then be managed independently. Particularly, their amplitude ratio and relative phase can take any value. The working frequency is not imposed by resonance conditions anymore, so a diminution of the dimensions of such a system does not come necessarily with an augmentation of this working frequency. Consequently, acoustic pressure, particle velocity and frequency can be easily and independently controlled in order to create an optimal acoustic field and to monitor it during the thermoacoustic process. Moreover, it must be emphasised that this kind of thermoacoustic device has the important advantage of being totally compact, meaning that its dimensions are roughly those of the stack, heat exchangers and loudspeakers set very closed together.

A view of the device used for experiments is shown in Fig. 8. This compact refrigerator consists of a cubic cavity filled with air at atmospheric pressure and at ambient temperature. A stack of parallel PVC plates is set in the cavity (note that this prototype does not comprise any heat exchanger). Two couples of face-to-face electrodynamic loudspeakers are used to generate the acoustic field. The electrical voltages supplied to the loudspeakers by four independent outputs of amplifiers are tuned in such a way that two face-to-face loudspeakers are supplied with electrical voltages in phase (then generating the pressure field) and that the two others are supplied with electrical voltages $\pi/2$ out of phase (then generating the velocity). Note that one loudspeaker only (instead of a couple) would be

(a) (b)

Fig. 8. Side view (a) and top view (b) of the experimental apparatus.

sufficient to generate the pressure field in the small cavity. The working frequency is chosen in such a way that the spacing between two plates of the stack is three times the thickness of the thermal boundary layer, which has been found to be the optimal stack spacing for thermoacoustic process in a standing wave resonator [12]. The thermo-physical and geometrical characteristics of the prototype are summarised in Table 1. The temperature distribution in the stack is measured by thermocouples spatially distributed on two plates located in the middle of the stack. The pressure in the cavity is measured by a microphone flush mounted on the centre of a wall of the cavity. The vibration velocities of the drivers membranes are measured using a laser vibrometer. The pressure measurements show that the acoustic pressure in the cavity is uniform with a discrepancy less than 1 dB.

For this prototype, the optimal amplitude of the particle velocity leading to a maximum temperature difference between the ends of the stack along the z-axis is $|u|_{\text{opt}} \approx 1.5\ \text{m s}^{-1}$ according to expression (21). Then, the membranes of the loudspeakers generating the particle velocity are driven in such a way that it fits this requirement. The membranes of the loudspeakers generating the pressure field are driven at their maximum linear excursion in order to create a maximum pressure level in the cavity, which is then $p \approx 150$ dB SPL.

For these given values of pressure level and amplitude velocity, the temperature difference between the ends of the stack along the z-axis is measured as a function of the relative phase between pressure and velocity. Fig. 9 shows the experimental results normalised by the maximal temperature difference obtained (which is equal to 7.5 K), as well as theoretical results, according to expression (18), normalised by the theoretical maximal value (which is equal to 32 K). There is a relatively good qualitative agreement between theoretical and experimental results, which particularly show the existence of an optimal phase leading to a maximal temperature difference. The experimental optimal phase $\phi_{\text{opt}} = -1.1$ rad corresponds to the theoretical one given by expression (22). However, the experimental temperature differences are about four times smaller than theoretical ones. This systematic discrepancy has already been reported in the case of a half-wave-

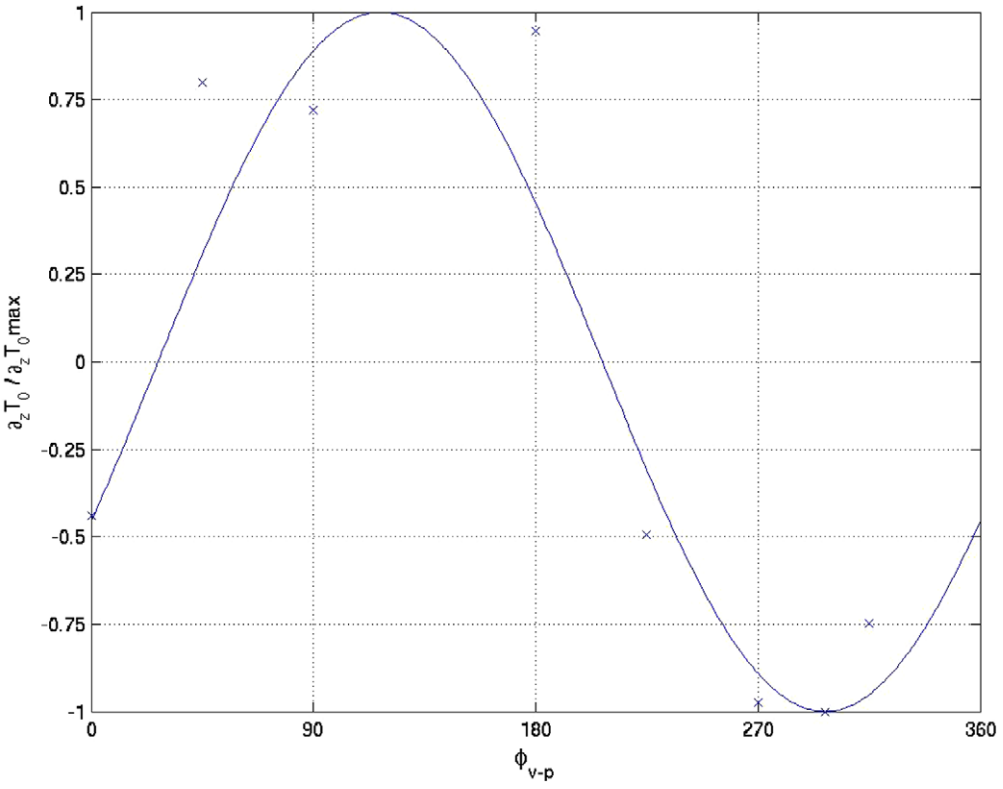

Fig. 9. Normalised temperature difference $\Delta T_0/\Delta T_{0\max}$ measured (×) and calculated (straight line) as a function of the phase ϕ_{v-p} between the particle velocity and the acoustic pressure. The maximal value of the experimental temperature difference is equal to $\Delta T_{0\max} = 7.5$ K, the maximal value of the calculated one is equal to $\Delta T_{0\max} = 31.9$ K. The geometrical and thermo-physical parameters of the thermoacoustic device are summarised in Table 1.

length resonator [13] and a recent numerical study proposes an explanation for this discrepancy [14].

It has to be noticed that the particle velocity along the x-axis close to the loudspeakers generating the pressure (which is here about 2.5 m s^{-1}) has the same order of magnitude as the optimal particle velocity generated along the z-axis. Thus, the parcels motion between two plates of the stack is not a rectilinear motion anymore, but an ellipsoidal one. Fig. 10 shows this ellipsoidal particle displacement measured in the compact device by mean of Laser Doppler Anemometry [15]. Then, the associated thermoacoustic heat transfer becomes a two-dimensional one and, consequently, the temperature difference is not necessarily established along the z-axis, as in a classical resonant thermoacoustic refrigerator. Moreover, this additional particle velocity along the x-axis leads to a significant additional global heating of the stack due to viscous dissipation. These effects have to be taken into account in order to improve the performances of future compact refrigerator prototypes.

Nevertheless, these first experimental results confirm that requirements that have to be taken into account in the design of thermoacoustic refrigerators can now be addressed, using theoretical results obtained in this work.

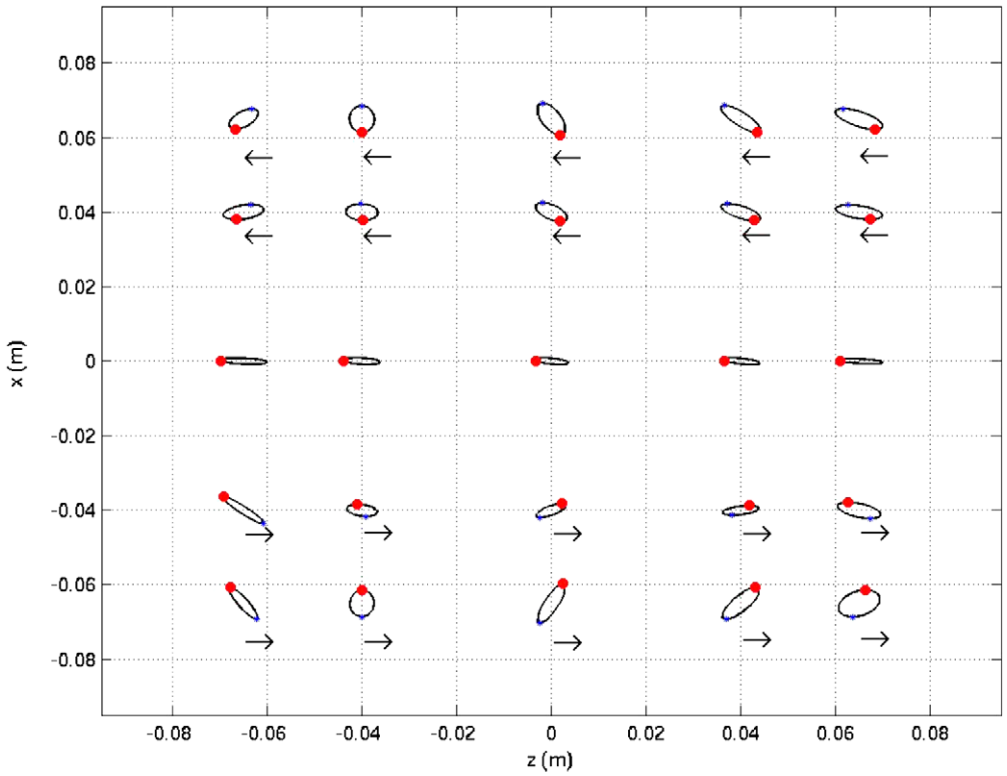

Fig. 10. Particle displacement during one period measured by mean of Laser Doppler Velocimetry in the plane $z = 0$ in the compact thermoacoustic device when the four acoustic sources are tuned to the optimal configuration. Arrows show the direction of the displacement.

6. Conclusion

The existence of an optimal acoustic field for thermoacoustic refrigeration has been shown, and optimal relationships between p, $|u|$ and ϕ which provide the maximal value of $\overline{Q}$ and $\partial_z T$ have been derived. This optimal field can be different from the one existing in usual standing wave thermoacoustic refrigerators, even if these refrigerators operate near the optimum in terms of the modulus of the particle velocity when a high drive ratio is reached. In particular, some improvements would be achieved in usual refrigerators by tuning the relative phase between acoustic pressure and particle velocity to its optimum (which is different to $\pi/2$).

A new kind of standing wave-like thermoacoustic refrigerator which allows generation of this optimal acoustic field in the stack has been designed. The original architecture of this device has the two following advantages: first, it allows independent control of the acoustic pressure and the particle velocity and, second, it leads to an extremely compact device.

However, further study has still to be carried out in order to precisely described the non-conventional two-dimensional behaviour of such a thermoacoustic device, and to improve its promised performances in terms of miniaturisation. Moreover, the loudspeak-

ers would be tuned in order to create an acoustic field which simulates inside the stack the behaviour of a travelling wave device. Then, the analysis presented in this paper would be extendable to an isothermal stack (regenerator in a Stirling engine), using the behaviour of the basic expressions of temperature gradient, heat flux and coefficient of performance for isothermal process.

References

[1] Ceperley PH. A pistonless stirling engine – the travelling wave heat engine. J Acoust Soc Am 1979;66:1508–13.
[2] Gusev V, Job S, Bailliet H, Lotton P, Bruneau M. Acoustic streaming in annular thermoacoustic prime-movers. J Acoust Soc Am 2000;108:934–45.
[3] Hofler TJ. Performance of a short parallel-plate thermoacoustic stack with arbitrary plate spacing. J. Acoust Soc Am 1990;88:594.
[4] Raspet R, Brewster J, Bass HE. A new approximation method for thermoacoustic calculations. J Acoust Soc Am 1998;103(5):2395–402.
[5] Petculescu G, Wilen LA. Alternative-geometry travelling wave thermoacoustic devices. In: First international workshop on thermoacoustics, Hertogenbosh, April 22–25 2001.
[6] Patent FR 03 05 982 (PCT WO 2004 10 20 84); 2003.
[7] Swift G. Thermoacoustic engines. J Acoust Soc Am 1988;84(4):1145–80.
[8] Wheatley J, Hofler T, Swift GW, Migiori A. An intrinsically irreversible thermoacoustic heat engine. J Acoust Soc Am 1983;74(1):153–70.
[9] Penelet G, Gaviot E, Gusev V, Lotton P, Bruneau M. Experimental investigation of transient non linear phenomena in an annular thermoacoustic prime-mover: observation of a doublethreshold effect. Cryogenics 2002;42:527–32.
[10] Atchley AA, Hofler TJ, Muzzerall ML, Kite MD. Acoustically generated temperature gradients in short plates. J Acoust Soc Am 1990;88(1):251–63.
[11] Bailliet H, Lotton P, Bruneau M, Gusev V. Coupling between loudspeakers and thermoacoustic cavities. Acta Acust 2000;86:363–73.
[12] Tijani MEH, Zeegers JCH, de Waele ATAM. The optimal stack spacing for thermoacoustic refrigeration. J Acoust Soc Am 2002;112(1):128–33.
[13] Kim YT, Suh SJ, Kim MG. Linear resonant duct thermoacoustic refrigerator having regenerator stack. In: 16th ICA, June 1998, p. 821–2.
[14] Marx D, Blanc-Benon Ph. Numerical calculation of the temperature difference between the extremities of a stack plate. Cryogenics 2005;45:163–72.
[15] Bailliet H, Lotton P, Bruneau M, Gusev V, Valiere JC, Gazengel B. Acoustic power flow measurement in a thermoacoustic resonator by means of L.D.A. and microphonic measurement. Appl Acoust 2000;60:1–11.